

## 18th CIRP Conference on Modeling of Machining Operations

## Effect of recirculation zone on debris evacuation during EDM deep hole drilling

Jibin Boban<sup>a\*</sup>, Afzaal Ahmed<sup>a</sup>, Ashwani Assam<sup>b</sup><sup>a</sup>Department of Mechanical Engineering, Indian Institute of Technology Palakkad, Kerala 678557, India<sup>b</sup>Department of Mechanical Engineering, Indian Institute of Technology Patna, Bihar 801106, India\* Corresponding author. Tel.: +91-04923-226432; fax: +91-04923-226300. E-mail address: [jibinboban143@gmail.com](mailto:jibinboban143@gmail.com)**Abstract**

Deep hole drilling is a technique used for producing holes in materials at high depth to diameter ( $L/D > 10$ ) ratios. Applications demanding deep holes can be extensively found in aerospace, automotive, marine and oil & gas industries. Conventional drilling techniques such as twist drilling and gun drilling are commonly used for drilling deep holes in the aforementioned applications. However, these methods can cause problems of rapid tool degradation, chip clogging, premature tool failure and undesirable sub-surface alterations to the hole surface. Moreover, these problems get aggravated when the material is difficult-to-cut (Ni/Fe/Co based superalloys) in nature. Therefore, non-conventional machining process finds scope in order to overcome the problems associated with conventional drilling. Electrical discharge drilling (EDD) can be used for fabricating dimensionally accurate holes irrespective of hardness of the material. Nevertheless, the inefficiency in flushing of debris particles at higher depths and its subsequent accumulation is a critical challenge during EDM deep hole drilling. The reason behind flushing inefficiency based on fluid physics has not been completely explored by researchers yet. In this paper, the flow behaviour of micro debris particles in the flushing channel during EDD has been analysed using CFD simulation by employing discrete phase modelling (DPM). The developed model set up is also validated with a benchmark fluid mechanics problem. The steady state CFD analysis results show the formation of multiple recirculation zones in the flushing channel. This can be attributed to the adverse pressure gradient experienced when the dielectric fluid passes from the machining gap to annular gap. Moreover, the presence of recirculation zones reduces the flow momentum and thereby debris particle velocity. This leads to accumulation of micro debris particles in the recirculation zones over time. The results also show that the trajectory of the particles is dependent on the size of the particles generated during material removal. The outcomes of numerical analysis in the present paper can serve as a foundation for the future studies in improving the performance of EDM deep hole drilling.

© 2021 The Authors. Published by Elsevier B.V.

This is an open access article under the CC BY-NC-ND license (<https://creativecommons.org/licenses/by-nc-nd/4.0>)

Peer-review under responsibility of the scientific committee of the 18th CIRP Conference on Modeling of Machining Operation.

*Keywords:* EDM; Debris; Recirculation zone; Drilling; Deep hole**1. Introduction****Nomenclature**

DPM	Discrete Phase Modelling
K	Turbulent Kinetic Energy
$\Omega$	Specific dissipation rate
SST	Shear stress transport
BFS	Backward Facing Step
$\mu$	Dynamic viscosity of fluid
$C_d$	Drag coefficient
RZ	Recirculation zone

Electrical discharge drilling (EDD) is an effective method for drilling holes in materials irrespective of their hardness. In EDD, the material removal occurs by means of pulsed electric discharges/sparks occurring between tool electrode and workpiece. The holes produced using EDD possess high dimensional accuracy and surface finish with tight tolerances. Therefore, EDD is widely employed in aerospace, automotive, biomedical, oil & gas and marine applications where surface finish and dimensional accuracy are vital. However, the inefficient flushing of debris particles and its accumulation at higher depths during EDD remains as a critical challenge. As a consequence, the accumulated debris particles result in secondary discharges / undesirable arcing

which causes tapering of the holes. Moreover, the frequent retractions of tool electrode due to accumulated debris leads to increase in overall machining time. Thus drilling deep holes using EDM is challenging. In order to overcome this issue, many researchers came up with different techniques with an aim to obtain high aspect ratio holes. These includes modifying tool electrode geometry, imparting rotation to tool electrode, executing electrode jump motion etc. Since most of these studies were carried out without understanding the fluid physics of debris motion, none of them could provide a complete solution. Therefore, attention is needed in exploring the flow behaviour within the flushing channel to overcome the challenges in EDD process.

## 2. Literature review on EDD and debris motion studies

### 2.1 Literature review on EDM deep hole drilling

The idea of employing EDM drilling for producing deep holes was of great interest to the researchers. In order to realize deep hole drilling using EDM, researchers proposed various methods. Kumar et al. [1] proposed a modified design by drilling an inclined hole through the tool electrode for conducting experiments on Ti6Al4V. The proposed electrode could successfully evacuate the debris particles with less sparking in the side gap and acted as a self-flushing electrode. The L/D ratio considered in the study was 12.25. In similar studies, tool electrode modifications were proposed by Nastasi et al. [2], Plaza et al. [3] and Wang et al. [4] where slotted tool electrodes were employed in EDD. These studies also reported better debris evacuation followed by improved MRR. However, it is well known that solid electrodes cannot reach the flushing efficiency of tubular tool electrodes in producing high aspect ratio holes. On the other hand, researchers also proposed a high speed rough drilling method called hybrid electrical discharge and arc machining (HEDAM) for fabricating deep holes in Inconel 718 [5,6]. However, this process requires a post processing method to achieve the desired quality of the hole. In a later work, Kuppan et al. [7] analysed the EDM deep hole profile in Inconel 718 where a wide mouth at the top, barrel shaped midway and a narrow region at the bottom was observed. He could also identify that secondary discharges and arcing during deep hole drilling were caused by debris particles in flushing channel. In another study, an attempt of employing low frequency vibration was put forward by Unune et al. [8] with a view to produce micro holes on Inconel 718. Results revealed that low frequency vibration improved MRR and reduced EWR, overcut and taper angle during micro EDD. Also, higher accuracy and better surface quality were achieved by the holes. This was mainly due to effective removal of debris from the gap and fresh continuous flow of dielectric into the IEG by employing low frequency vibration. However, the aspect ratio of holes considered in this study was only 5. Apart from this, Ahmed et al. [9] attempted to introduce a novel deep hole drilling method for Inconel by combining EDM drilling and conventional drilling methods. The method involves fabricating a straight guide hole using EDD followed by conventional gundrilling process. Anyhow, EDD has to depend on an additional drilling method for

realizing deep hole fabrication. From the aforementioned studies, it is evident that the solutions proposed by researchers for deep hole drilling using EDM is very limited. In order to come up with a suitable solution, researchers started to explore the underlying reason behind the ineffective debris removal in EDD by studying the debris flushing phenomena.

### 2.2 Literature review on flushing flow analysis and debris motion studies in EDD

Rajurkar et al. [10] initiated the studies related to debris particles produced in EDM process by developing a theoretical background for debris formation and ejection mechanism. Followed by this, Cetin et al. [11] conducted a numerical study to analyse debris motion and distribution during various levels of electrode jump motion. The results showed that the concentration of debris particles at machining gap corners results in localized secondary discharges leading to the concavity of holes. In another study, Wang et al. [12] attempted simulating liquid-solid two phase flow field within the discharge gap during high speed small hole EDM drilling. The material removal rate (MRR) was found to decrease with the increase in drilling depth. In a similar work, researchers performed numerical simulation of debris particle motion in micro EDM deep hole drilling by considering electro viscous effect [13]. The study concluded that the concentration of debris particles at the corner of machining gap leads to secondary discharges and corner wear on tool electrode. Later on, a computational model was also developed by Arvind et al. [14] to explore debris flushing phenomena in spray EDM technique. The model could provide close agreement with experimental results in predicting the debris distribution percentage along the crater. In order to improve the existing numerical studies for debris motion, a flow field model was proposed by including bubble as a third phase other than debris and dielectric medium [15]. The work revealed that the bubble expansion within the machining gap also influence the exclusion of debris from the gap. Further, Wang et al. [16] applied the same three phase flow to estimate the debris and bubble behaviour during electrode jump motion. The mixing of debris with clean EDM oil was evident during electrode jump up motion and the mixture gets expelled out during jump down motion. In addition to these studies, Kliuev et al. [17] conducted CFD simulations to study the variation in pressure drop and dielectric flow pattern during EDM drilling by employing single channel and multi-channel configurations of tool electrode. Single channel electrodes exhibited efficient flushing capability and effective debris removal compared to smaller diameter electrodes and multi-channel electrodes. Kliuev et al. [18] also investigated the flow behaviour of dielectric medium during machining inside a predrilled hole using CFD analysis and particle tracking velocimetry. The debris particle motion was found to slow down during hole drilling process compared to the motion during planar surface machining. Thus debris particles gets flushed out with delay during deep hole drilling using EDM. However, the reason behind reduction in debris particle velocity was not discussed. Besides these, Tanjilul et al. [19] developed a CFD model that can predict the trajectory of the debris particles during flushing flow of dielectric medium. The proposed model can be utilized for analysing the flushing effectiveness of drilling electrodes with varying geometry.

The study could also come up with an incremental improvement in debris evacuation efficiency using vacuum assistance during EDM drilling. Feng et al. [20] also developed a model to investigate the effects of tool electrode rotation in debris particle motion during side nozzle flushing. The study established that the removal of debris particles was effective when the tool electrode is subjected to higher rotating speeds.

Although many researchers have explored the debris motion in the flushing channel through various methods, limited studies have been carried out in exploring the phenomena of debris accumulation based on fluid dynamics approach. In this paper, an investigation into the fluid flow behaviour of dielectric fluid and motion of micro debris particles in the flushing channel are analysed at 100 mm depth of EDM drilling by employing an appropriate CFD model.

### 3. Dielectric and debris flushing simulation

#### 3.1. Mathematical basis of flushing model

In flushing flow numerical simulation, the dielectric fluid is treated as continuous phase while debris particles are considered as discrete phase. The continuous phase flow field is solved by coupling the continuity equation and Navier-Stokes equations. The trajectory of micro debris particles are obtained by solving the particle force balance equation in Lagrangian reference frame.

$$\frac{dV_p}{dt} = F_d(V_f - V_p) + g\left(\frac{\rho_p - \rho_f}{\rho_p}\right) + F \quad (1)$$

where  $F_d(V_f - V_p)$  and  $F$  represents the drag force and additional acceleration forces experienced per unit mass of the particle respectively. The velocities of fluid phase and debris particles are represented respectively by  $V_f$  and  $V_p$  while  $\rho_f$  and  $\rho_p$  represents their densities. The term  $F_d$  is given by

$$F_d = \frac{18\mu C_d (Re)_{rel}}{\rho_p d_p^2 24} \quad (2)$$

where  $\mu$  is the dynamic viscosity of the fluid,  $C_d$  is the drag coefficient and  $(Re)_{rel}$  is the relative Reynolds number given as

$$(Re)_{rel} \equiv \frac{\rho_p d_p |V_p - V_f|}{\mu} \quad (3)$$

Equation 1 is integrated with respect to time to obtain the velocity of the debris particle at each point along the trajectory. The trajectory itself is predicted by

$$\frac{dx_p}{dt} = V_p \quad (4)$$

Equation 4 is solved simultaneously along with equation 1 to determine the velocity and position of the particle at a given instant.

#### 3.2. Numerical modelling

The numerical model was developed using ANSYS Fluent 18.2 for establishing the flow behaviour of dielectric and motion of the micro debris particles. A 2-D axisymmetric geometry of a tubular tool electrode configuration having 3.5

mm outer diameter was used for performing flushing simulations. The width of the machining gap and side annular gap was fixed as 200  $\mu\text{m}$  and 500  $\mu\text{m}$  respectively. Annular gap represents the overcut in EDD between tool electrode and the workpiece. The geometrical configuration and boundary conditions employed for the simulation is shown in Fig.1.

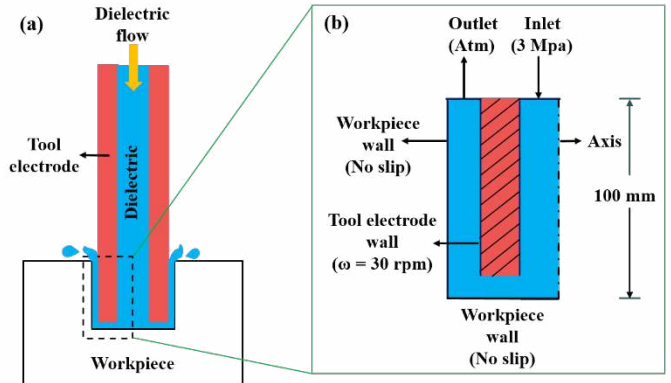


Fig.1. (a) Schematic of EDM hole drilling and (b) geometrical model with boundary conditions

Discrete phase modelling (DPM) is chosen to incorporate the injection of micro debris particles during flushing flow. Semi-implicit method for pressure linked equations (SIMPLE) algorithm was selected for solving the flow field. The turbulence model chosen was  $k-\omega$  SST model as it is typically better in predicting adverse pressure gradient boundary layer flows and separation. The typical size of debris particles generated during EDM will be in the range of  $\sim 1$  to 100  $\mu\text{m}$ . In the present model, group injection of particles is employed with particle sizes varying from 1 to 70  $\mu\text{m}$ . The particles are injected within the machining gap based on Rosin Rammler distribution where equal weightage was assigned to all particle sizes. The tool electrode wall is provided with rotating wall boundary condition with a rotational speed of 30 rpm (3.1416 rad/s). The details of the numerical model is shown in Table 1.

Table 1. Numerical model details and conditions

Details	Conditions
Geometry	2D - Axisymmetric
Dielectric medium	Deionised water
Debris particle material	Steel
Turbulence model	$K-\omega$ SST
Flushing type	Tubular flushing
Flushing pressure (MPa)	3
Drilling depth (mm)	100

#### 3.3. Mesh independence study

Prior to CFD simulations, mesh independence study was carried out with an aim to obtain reliable and accurate results. Geometry creation and meshing was done in ICEM CFD with a spacing of  $10^{-7}$  m at the walls. Meshing done at the machining gap was refined subsequently in order to make the results mesh independent and to effectively capture the flow field over 200  $\mu\text{m}$  region. Quadrilateral cells were employed to ensure better convergence and accuracy. The total cells for coarse, medium and fine mesh resolution were taken as

45476, 129901 and 209100 respectively. From this study, medium mesh resolution was fixed which could predict the velocity profile same as that of a finer mesh as shown in Fig.2.

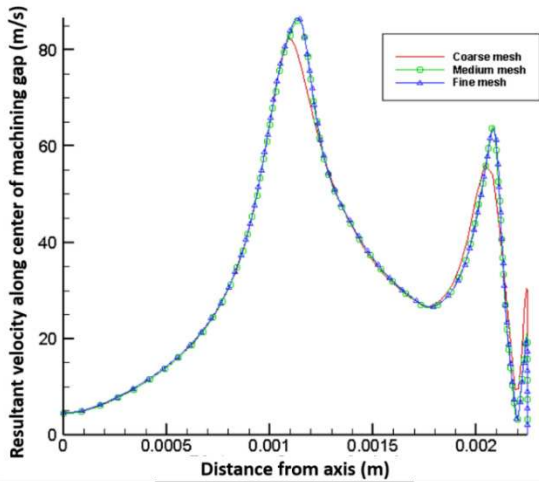


Fig.2. Mesh independence study

### 3.4. Simulation procedure

Mesh for the geometry created in ICEM CFD is imported into ANSYS Fluent 18.2 for performing simulation. Initially, the continuous phase flow field is solved without the injection of particles until the flow attains steady state. The convergence criteria was set to relative residual value less than  $10^{-6}$  for both mass conservation and momentum balance equations. Once the steady state has been achieved by the fluid phase, group injection with 1000 particle stream is employed over the machining gap at intervals of  $30 \mu s$ . The simulation is carried out for 1 ms time period to analyse the motion of micro debris particles across the flushing channel.

## 4. Results and discussions

### 4.1 Validation with benchmark problem

The numerical modelling set up was first validated with a problem involving particle injection through a backward facing step (BFS). The BFS is a widely used benchmark problem in fluid mechanics which involves flow separation and recirculation. In BFS, the fluid flow is subjected to a sudden enlargement of cross-sectional area leading to separation of flow starting at the expansion point.

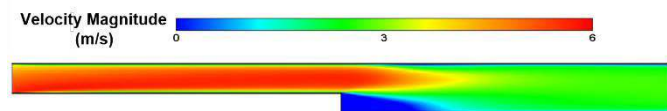


Fig. 3. Velocity contour for BFS

The validation was carried out by employing a similar model setup used for the current study in solving the flow over a backward facing step and comparing it with the numerical results obtained by Lu et al. [21] and experimental results obtained by Fessler et al. [22] at  $x/H = 5$ . The benchmark BFS problem involves turbulent flow with micron sized particles in the fluid domain. The velocity contour for

the flow through BFS is shown in Fig.3. The obtained results were found to be in close agreement with the results obtained from previous works as shown in Fig. 4. The abscissa represents dimensionless value which is the ratio of velocity at the point being measured ( $U$ ) to the free stream velocity ( $U_0$ ) while ordinate represents the ratio of height of the point ( $y$ ) to the height of backward facing step ( $H$ ).

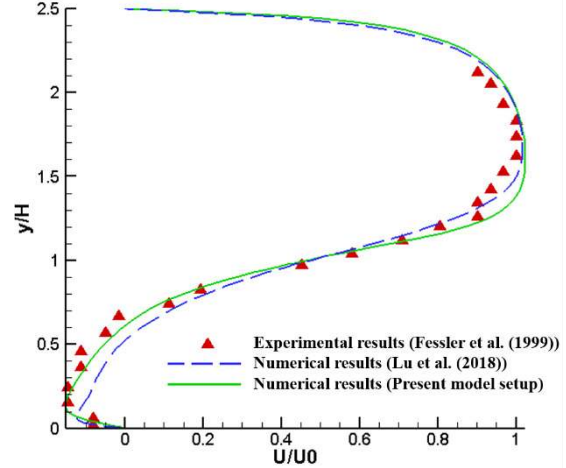


Fig. 4. Validation of results

### 4.2 Steady state analysis

The steady state condition for the continuous phase flow exhibits the presence of multiple recirculation zones (separation bubble) within the flushing channel. These include one bigger recirculation zone (zone 1) nearer to the bottom edge of tool electrode and two smaller recirculation zones (zone 2 and zone 3). The recirculation zones (RZ) formed during continuous phase flow is shown in Fig.5.

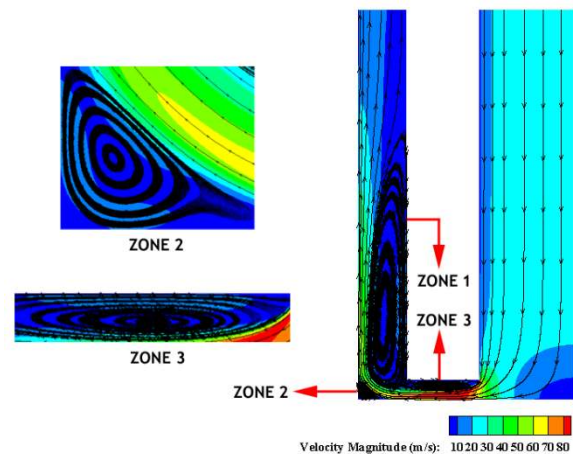


Fig. 5. Velocity contour and recirculation zones in flushing channel

The formation of recirculation zones is mainly due to the adverse pressure gradient that occurs when the flow changes its direction abruptly from its normal path. The fluid nearer to the wall cannot overcome the adverse pressure gradient generated due to sharp bend in the flushing channel. This leads to a separation of flow from the boundary resulting in the formation of recirculation zones. The characteristic dimensions of larger RZ (zone 1) are highlighted in Fig.6. Reattachment length (RL) represents the distance from the

point of separation to the point where the flow resumes its intended path all over the cross section. The thickness of larger RZ ( $t$ ) and RL are provided in Table 2.

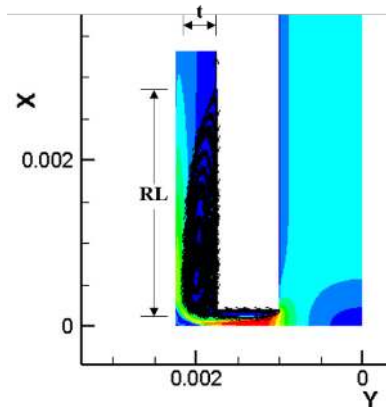


Fig.6 Characteristic dimensions of larger RZ (zone 1)

Table 2. Characteristic dimensions of RZ

Features	Dimensions
Thickness of zone 1 ( $t$ )	~ 400 $\mu\text{m}$
Reattachment length (RL)	~ 2.8 mm

### 4.3 Effect of recirculation zone (RZ)

The particles injected at the machining gap was found to trace the streamlines of the continuous phase. Some of the particles get trapped inside the larger RZ in the annular gap as well as in the smaller RZ at the corner and loops around within the zone. As injection continues for every pulse on time, more and more particles enter the recirculation zone resulting in the accumulation of the debris particles. The range of particle diameter used in Fig. 7 is between 1 to 50  $\mu\text{m}$  with a mean diameter of 25  $\mu\text{m}$ . The increase in accumulation of debris particles at the recirculation region can be observed with increase in time qualitatively at levels of 200  $\mu\text{s}$ , 400  $\mu\text{s}$  and 600  $\mu\text{s}$  as shown in Fig. 7.

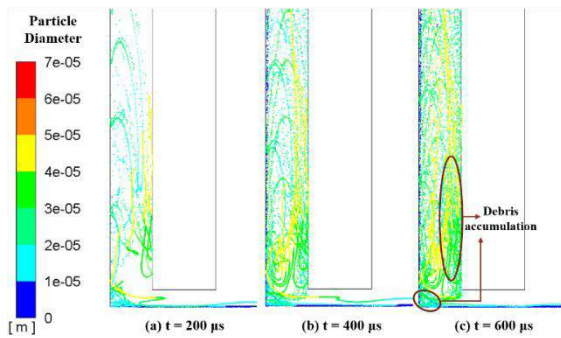


Fig. 7. Effect of recirculation zones

It can also be observed from Fig. 8 that the velocity is dropping significantly when the flow approaches major RZ in the annular gap. The adverse pressure gradient resulting from change in flow direction causes flow separation. This results in the formation of turbulent eddies by which the dielectric fluid experiences loss in momentum. Thus velocity is not elevated further after momentum loss in major RZ. As a consequence, the debris particles are not flushed out effectively at higher depths.

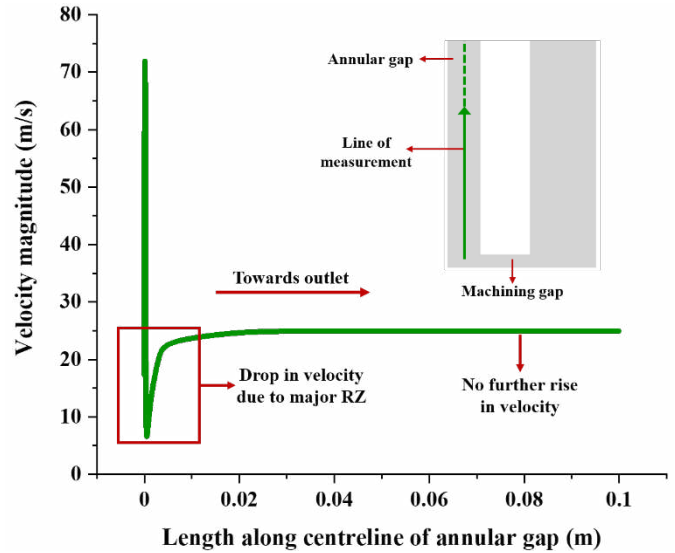


Fig.8. Velocity drop due to major RZ

### 4.4 Effect of particle size

The trajectory of particles during flushing is very much dependent on the size of the individual particles as shown in Fig. 9. The injections are performed with varying ranges of particle diameters such as from 1 to 10  $\mu\text{m}$ , 1 to 30  $\mu\text{m}$ , 1 to 50  $\mu\text{m}$  and 1 to 70  $\mu\text{m}$  with mean diameters of 5  $\mu\text{m}$ , 15  $\mu\text{m}$ , 25  $\mu\text{m}$  and 35  $\mu\text{m}$  respectively. The particles with smaller diameters in the range of 1 to 10  $\mu\text{m}$  seems to move rapidly along the annular channel without entering the recirculation zone as shown in Fig. 9 (a). Due to the momentum attained by their lighter mass, they are forced to move closer to the outer walls and flow through the region having higher velocity magnitude.

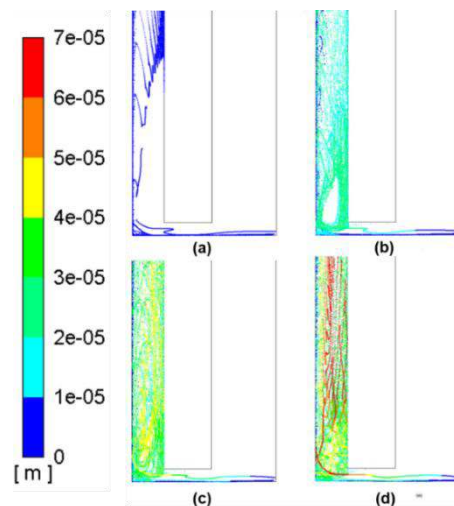


Fig. 9. Effect of variation in particle sizes (a) 1 to 10  $\mu\text{m}$  (b) 1 to 30  $\mu\text{m}$  (c) 1 to 50  $\mu\text{m}$  and (d) 1 to 70  $\mu\text{m}$

When particle diameter increases in the range between 1 to 30  $\mu\text{m}$ , the particles start entering the outer periphery of the recirculation zone as shown in Fig. 9 (b). The entire recirculation zone is filled by the particles when the diameter range becomes 1 to 50  $\mu\text{m}$  as shown in Fig. 9 (c). This is because the velocity attained by the intermediate sized

particles (Fig. 9 (b) and (c)) will be less compared to smaller sized particles and will be almost equivalent to the velocity within the recirculation region. Hence they are forced to follow the stream lines of recirculation zone after the collision with either smaller particles or wall and tend to enter the recirculation zone. But as the diameter range becomes 1 to 70  $\mu\text{m}$ , it can be observed that larger particles entering the outer periphery of recirculation zone is forced to go out as shown in Fig. 9 (d). This can be attributed to the high centrifugal force experienced by the larger mass of the particles and the interplay among drag force and gravity forces.

## 5. Conclusions

The following conclusions can be derived from the present study:

1. The validation results using BFS by incorporating the proposed model setup shows close agreement with the results from previous numerical and experimental studies. This substantiates the validity of the proposed numerical model and reliability of simulation results.
2. The steady state analysis shows the presence of multiple recirculation zones in the flushing channel formed due to the adverse pressure gradient experienced during the flow. The extent of major RZ is significant in annular gap such that it reduces the flow velocity significantly and slows down debris motion.
3. The presence of recirculation zones in the flushing channel traps the debris particles, especially intermediate sized particles. Thus the particles lose their momentum and gets accumulated within these zones. More and more particles would accumulate in due course of time with continuous material removal leading to secondary discharges causing wear at the corner of the tool electrode.
4. Although larger particles enter the recirculation zones, the higher centrifugal force generated due to their greater mass and/or the interplay between gravity and drag forces expels them out of the recirculation zone.

The outcomes of present study can certainly uplift the research in proposing innovative solutions for producing high aspect ratio holes using EDD. However, the present study considers DPM modelling in which particles are considered only as point masses. Moreover, the future work will be focussed on eliminating recirculation zones that ultimately ensures realization of deep hole drilling through efficient debris evacuation.

## Acknowledgements

The authors are grateful to the Indian Institute of Technology (IIT) Palakkad for providing suitable numerical simulation environment (ANSYS Fluent 18.2 software).

## References

- [1] Kumar, R., Singh, I. A modified electrode design for improving process performance of electric discharge drilling. *Journal of Materials Processing Technology*. 2019; 264:211-219.
- [2] Nastasi, R., Koshy, P. Analysis and performance of slotted tools in electrical discharge drilling. *CIRP Annals*. 2014; 63(1), 205-208.
- [3] Plaza, S., Sanchez, J. A., Perez, E., Gil, R., Izquierdo, B., Ortega, N., & Pombo, I. Experimental study on micro EDM-drilling of Ti6Al4V using helical electrode. *Precision Engineering*. 2014; 38(4), 821-827.
- [4] Wang, K., Zhang, Q., Zhu, G., Liu, Q., & Huang, Y. Experimental study on micro electrical discharge machining with helical electrode. *The International Journal of Advanced Manufacturing Technology*. 2017; 93(5-8), 2639-2645.
- [5] Ahmed, A., Tanjilul, M., Fardin, A., Wong, Y. S., Rahman, M., & Kumar, A. S. On the design and application of hybrid electrical discharge and arc machining process for enhancing drilling performance in Inconel 718. *The International Journal of Advanced Manufacturing Technology*. 2018; 99(5-8), 1825-1837.
- [6] Ahmed, A., Tanjilul, M., Rahman, M., & Kumar, A. S. Ultrafast drilling of Inconel 718 using hybrid EDM with different electrode materials. *The International Journal of Advanced Manufacturing Technology*. 2020; 106(5), 2281-2294.
- [7] Kuppan, P., Narayanan, S., Rajadurai, A., & Adithan, M. Effect of EDM parameters on hole quality characteristics in deep hole drilling of Inconel 718 superalloy. *International Journal of Manufacturing Research*. 2015; 10(1), 45-63.
- [8] Unune, D. R., Nirala, C. K., & Mali, H. S. Accuracy and quality of micro-holes in vibration assisted micro-electro-discharge drilling of Inconel 718. *Measurement*. 2019; 135, 424-437.
- [9] Ahmed, A., Lew, M. T., Divakar, P., Kumar, A. S., & Rahman, M. A novel approach in high performance deep hole drilling of Inconel 718. *Precision Engineering*. 2019; 56, 432-437.
- [10] Rajurkar KP, Pandit SM. Formation and ejection of EDM debris. *J. Eng. Ind. Trans. ASME*. 1986; 108: 22-26.
- [11] Cetin S, Okada A, Uno Y. Effect of debris distribution on wall concavity in deep-hole EDM. *JSME International Journal Series C Mechanical Systems, Machine Elements and Manufacturing*. 2004; 47(2):553-559
- [12] Wang YQ, Cao MR, Yang SQ, Li WH. Numerical simulation of liquid-solid two-phase flow field in discharge gap of high-speed small hole EDM drilling. *Advanced Materials Research*. Trans Tech Publications Ltd. 2008; 53:409-414.
- [13] Wang J, Wang YG, Zhao FL. Simulation of debris movement in micro electrical discharge machining of deep holes. *Materials Science Forum*. Trans Tech Publications Ltd. 2009; 626:267-272
- [14] Pattabhiraman A, Marla D, Kapoor SG. A computational model to study film formation and debris flushing phenomena in spray-electric discharge machining. *Journal of Micro and Nano-Manufacturing*. 2016; 4(3).
- [15] Wang J, Han F. Simulation model of debris and bubble movement in consecutive-pulse discharge of electrical discharge machining. *International Journal of Machine Tools and Manufacture*. 2014; 77:56-65.
- [16] Wang J, Han F. Simulation model of debris and bubble movement in electrode jump of electrical discharge machining. *The International Journal of Advanced Manufacturing Technology*. 2014; 74(5-8):591-8.
- [17] Kliuev M, Baumgart C, Büttner H, Wegener K. Flushing velocity observations and analysis during EDM drilling. *Procedia CIRP*. 2018; 77:590-3.
- [18] Kliuev M, Baumgart C, Wegener K. Fluid Dynamics in electrode flushing channel and electrode-workpiece gap during EDM drilling. *Procedia CIRP*. 2018; 68:254-9.
- [19] Tanjilul M, Ahmed A, Kumar AS, Rahman M. A study on EDM debris particle size and flushing mechanism for efficient debris removal in EDM-drilling of Inconel 718. *Journal of Materials Processing Technology*. 2018; 255:263-74.
- [20] Feng G, Yang X, Chi G. Experimental and simulation study on micro hole machining in EDM with high-speed tool electrode rotation. *The International Journal of Advanced Manufacturing Technology*. 2019; 101(1-4):367-75.
- [21] Lu H, Zhao W. Numerical study of particle deposition in turbulent duct flow with a forward-or backward-facing step. *Fuel*. 2018; 234:189-98.
- [22] Fessler JR, Eaton JK. Turbulence modification by particles in a backward-facing step flow. *Journal of Fluid Mechanics*. 1999; 394:97-111